First-Order PMD Outage for the Hinge Model

H. Kogelnik, *Life Fellow, IEEE*, P. J. Winzer, *Member, IEEE*, L. E. Nelson, *Member, IEEE*, R. M. Jopson, *Member, IEEE*, M. Boroditsky, *Senior Member, IEEE*, and M. Brodsky

***Abstract*—System outage due to first-order polarization-mode dispersion of links obeying the hinge model is analyzed using outage maps. We find that some fraction of the wavelength-division-multiplexed fiber capacity does not meet any outage specification.**

***Index Terms*—Optical fiber communication, outage probability, polarization-mode dispersion (PMD).**

I. Conceptual Background

POLARIZATION-MODE dispersion (PMD) measurements of deployed fiber plant [1]–[3] show that typical transmission links consist of several stable long fiber sections well sheltered from the environment over extended periods of time (months). On these time scales, the PMD characteristics of these sections are not impacted by temperature variations or mechanical vibrations. The stable fiber sections are connected by pieces of environmentally unprotected fiber "hinges" such as dispersion-compensating modules at repeater sites. The polarization characteristics of the hinges vary rapidly in time. A "hinge model" has been proposed [4], [5] to characterize the PMD statistics of such fiber links. It assumes that the hinges act as polarization transformers producing uniform coverage of the Poincaré sphere. The differential group delay (DGD) of the long sections has Maxwellian probability density (PDF) in the wavelength dimension, but is essentially frozen in time. Here we re-examine the traditional concepts of transmission system outage due to PMD [6], [7] in the light of the hinge model, and apply first-order outage maps [8], [9] to the model.

Assuming beat-noise-limited systems, and using the outage map approach, one determines optical signal-to-noise ratio (OSNR) penalties by experiment, simulation, or analysis. The OSNR needed for a given bit-error ratio (BER) in the absence of PMD is used as a base line. The OSNR penalty is then defined as the increase in OSNR needed to restore the BER to its previous value in the presence of PMD. The OSNR penalty is a function of the instantaneous DGD as well as of the polarization launch relative to the fiber's principal state of polarization (PSP), and depends on modulation format, bit rate, and receiver parameters [7], [9]. In a transmission system, the link's DGD, τ, as well as the PSPs fluctuate stochastically with time. In order to avoid excessive error bursts due to severe signal distortions, system designers allocate an OSNR margin (typically 1 or 2 dB). An outage occurs when the PMD induced penalty exceeds the allocated margin.

Manuscript received December 17, 2004; revised February 11, 2005.

H. Kogelnik, P. J. Winzer, and R. M. Jopson are with Bell Laboratories, Lucent Technologies, Murray Hill, NJ 07974 USA (e-mail: herwig@lucent.com).

L. E. Nelson is with OFS Laboratories, Somerset, NJ 08873 USA.

M. Brodsky and M. Boroditsky are with AT&T Laboratories—Research, Middletown, NJ 07748 USA.

Digital Object Identifier 10.1109/LPT.2005.846940

Within the confines of the hinge model, the hinges are the sole cause of the temporal fluctuations of the link's DGD, whereas, the DGD values of each section are fixed in time but are different for each statistically independent wavelength band. Bands may contain one *or more* wavelength-division-multiplexed (WDM) channels and are considered statistically independent when their spectral separation exceeds six times the bandwidth of the PSP of a *section* [6]. Consequently, for a time period over which the section DGDs remain constant, each band has a different outage probability $P_{\rm out}$ [4], [5], depending on its random but quasi-static section-DGD values. Some bands exhibit higher outage probabilities than others, and will, therefore, not comply with a prescribed outage specification. Thus, compared to traditional PMD outage statistics, where all WDM channels show identical outage probabilities, we have an additional parameter: the fraction of the WDM fiber spectrum that is noncompliant with a given outage specification, which we call the noncompliant capacity ratio (NCR).

Our goal is to determine the relationship among mean fiber DGD $\overline{\Delta\tau}$, specified outage probability $P_{\rm spec}$, and NCR for a given number of hinges. We choose five hinges as a typical example. The case of an infinite number of hinges is covered by the traditional analysis, where all bands experience the same outage probability, and NCR is either zero (if $P_{\rm out} < P_{\rm spec}$) or one (if $P_{\rm out} > P_{\rm spec}$).

II. Outage Weight and Outage Probability

An outage map plots contours of constant OSNR penalty as a function of τ and γ, the power splitting ratio [9]. To obtain the outage probability $P_{\rm out}$, one integrates the PDFs of τ and γ over the portion of the map exceeding the specified margin M (here, $M = 1$ dB). The PDF $P_{\rm DGD}$ of τ is a Maxwellian in the traditional case, but needs to be specially evaluated for the hinge model [4], [5]. Integration over the uniform γ gives [9]

$$P_{\rm out} = \int P_{\rm DGD}(\tau)\Delta\gamma(\tau)d\tau \tag{1}$$

where the outage weight $\Delta\gamma(\tau)$ is the range of γ for which the OSNR penalty exceeds M. A typical shape of $\Delta\gamma(\tau)$ is shown in Fig. 1. Note the cutoff at τ_0, below which no signal launch polarization can produce penalties exceeding M.

As an example, assume a link with $\overline{\Delta\tau} = 3$ ps consisting of six sections (i.e., five hinges) of equal mean DGD. For each band, the DGD values of each section are randomly determined from a Maxwellian. For two selected bands, the sets of DGD values are shown in Fig. 1 ranging from 0.55 to 1.62 ps for Band A, and 0.77 to 2.43 ps for Band B. For the PDFs of τ of these bands, analytical expressions were reported in [10]. They are shown in Fig. 1. Note that these PDFs have an upper cutoff; their

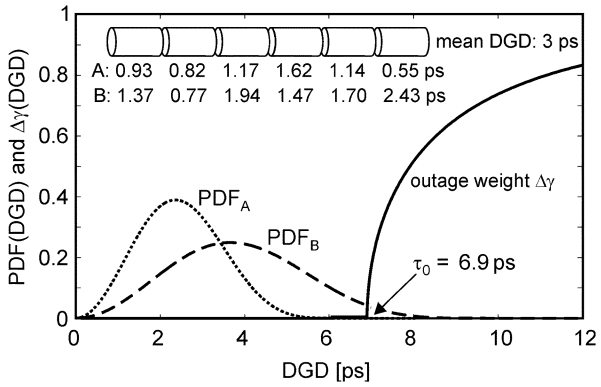

Fig. 1. Outage weight for NRZ modulation at 40 Gb/s and DGD densities for two illustrative frequency bands as a function of τ. The section DGD values for the bands are in the figure. There is no overlap between $\Delta\gamma$ and the PDF of the outage-free Band A.

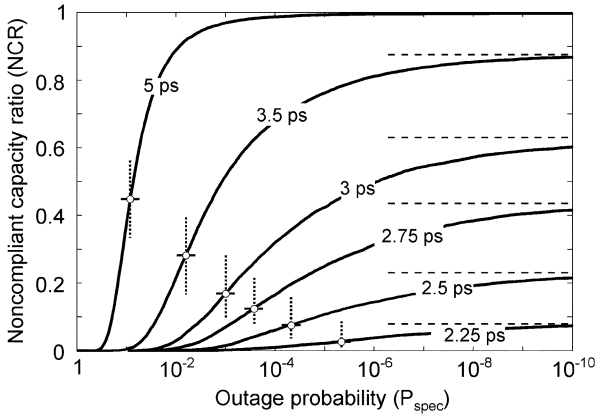

Fig. 2. NCR as a function of $P_{\rm spec}$ for links with five hinges, 1-dB margin, and 40-Gb/s NRZ modulation. The link's mean DGD is indicated on each curve. The dotted lines indicate the traditional outage probabilities obtained by using [7, eq. (4)]. The dashed horizontal lines are the asymptotes of zero outage probability for each mean DGD.

maximum DGD equals the sum of the section DGDs. Using (1), we find $P_{\rm out} = 8.5 \times 10^{-3}$ for Band B. Since the cutoff for PDF$_A$ is smaller than τ_0, Band A is outage-free ($P_{\rm out} = 0$).

III. Noncompliant Fiber Capacity

We proceed to determine how $\overline{\Delta\tau}$, $P_{\rm spec}$, and NCR are related for links of five hinges. To this end, we repeat the procedure described above for 10 000 bands. The resulting distribution of 10 000 $P_{\rm out}$-values allows us to determine the NCR for different outage specifications $P_{\rm spec}$. This procedure is then repeated for different values of $\overline{\Delta\tau}$.

The required $\Delta\gamma(\tau)$ of a typical receiver was determined from simulations [11], using a $2^7 - 1$ pseudorandom bit sequence, Gaussian detection statistics, a second-order Gaussian optical filter (3-dB bandwidth $2.2/T$), and a fifth-order Bessel electrical filter (bandwidth $0.6/T$), where T is the bit interval. The OSNR penalties were simulated as a function of τ and γ for nonreturn-to-zero (NRZ) and 33% duty cycle return-to-zero (RZ) at 40 Gb/s and 10^{-10} BER. The simulations showed that penalties and outage weight are well represented by the modified-quadratic approximation used in (3) of [7] giving

$$\Delta\gamma(\tau) = \sqrt{\frac{1+4\alpha M}{A}}\sqrt{1-\left(\frac{\tau_0}{\tau}\right)^2} \qquad (2)$$

where $\tau_0 = 2T/\sqrt{A/M+4\alpha}$ is the $\Delta\gamma$-cutoff mentioned above. The parameters obtained for the two chosen modulation formats were $A = 13$, $\alpha = 1.04$ for RZ, and $A = 51$, $\alpha = 0.41$ for NRZ. Above $\tau = \tau_{\rm MAX} = T/\sqrt{\alpha}$, we set $\Delta\gamma(\tau) = 1$ reflecting its physical bound. We used these values together with (1) and (2) for the computation of NCR. The results for NRZ and a selected number of mean DGDs are shown in Fig. 2, where NCR is plotted as a function of specified outage. Plots for RZ look similar except that corresponding mean DGDs are about twice as large. Upper bounds for $P_{\rm out}$ can be estimated by assuming polarization-independent penalties and setting $\Delta\gamma = 0$ below τ_0 and $\Delta\gamma = 1$ above it, as in [5].

IV. Discussion

Compare the results shown in Fig. 2 for the hinge model with the traditional results corresponding to an infinite number of hinges. For the latter, there is a distinct outage probability, marked by a vertical dotted line, for each specified mean DGD, marked by an open circle. In the traditional case, all spectral bands have the same outage characteristics. For a given mean DGD, e.g., 2.5 ps, all bands will either satisfy a specified outage, or all bands will violate it. There will be an abrupt transition from NCR $= 0$ to NCR $= 1$. This transition occurs at the outage value marked by the dotted line, i.e., all bands are guaranteed an outage probability of less than about 5×10^{-5} as long as $\overline{\Delta\tau} = 2.5$ ps or less. As the number of hinges increases from the five-hinge case discussed below, the NCR curves get steeper and approach the vertical dotted lines.

In systems characterized by the hinge model, the NCR for a given mean DGD undergoes a gradual transition from zero to a zero-outage asymptote, as shown in Fig. 2. This means that the specified outage with given mean DGD cannot be guaranteed for all bands. For the example of 2.5 ps and the 5×10^{-5} outage specification, we see that about 8% of the bands will violate that specification. Lower mean DGDs will decrease NCR, but only gradually. As a consequence of the gradual transition, there exist some bands satisfying the specified outage in the parameter range to the right of the dotted line, where all bands would have violated the outage specification in a traditional link. In fact, some bands are totally outage-free, as in the example of Band A of Fig. 1. An outage-free band occurs when the sum of all its section DGDs is smaller than the cutoff τ_0.

The case of zero outage is an interesting asymptote for our data. Its probability can be calculated from the Maxwellians $P_{\rm SECT}$ of the individual sections. For N sections of equal mean DGD, the PDF of the sum is $F^{-1}(F(P_{\rm SECT}))^N$, where F indicates a Fourier transform operation. The cumulative probability for sums smaller than τ_0 is the probability of outage free bands. The corresponding asymptotes NCR$_0$ for the NCRs are entered as horizontal dashed lines in Fig. 2. We find

$$\mathrm{NCR}_0 \approx 0.5\mathrm{erfc}\left(\frac{2\left(\frac{\tau_0}{\overline{\Delta\tau}} - \sqrt{N}\right)}{\sqrt{3\pi - 8}}\right) \qquad (3)$$

obtained from the central limit theorem, to be an excellent approximation for NCR$_0$, in agreement with [12].

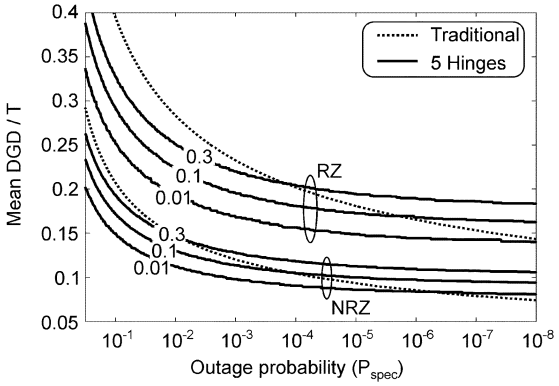

Fig. 3. Mean DGD/T of the link required for specified outage probability for links with five hinges, 1-dB OSNR margins, and the NRZ and RZ formats. Contours for NCR $= 0.01, 0.1,$ and 0.3 are shown. The traditional outage curves are dashed.

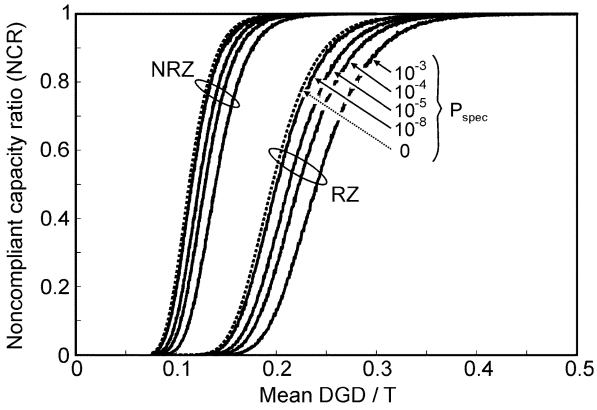

Fig. 4. Noncompliant fiber capacity versus mean DGD/T of the link for specified values of the outage probability for links with five hinges, 1-dB OSNR margins, and the NRZ and RZ formats.

The fact that the hinge model predicts some bands that are "outage free" at first might seem advantageous for system designers. However, the existence of noncompliant bands presents new difficulties as they must either take these bands out of service and use spare bands combined with protection switching, or employ other techniques of PMD mitigation. Note that this problem occurs even for DGD and outage parameters where for classical systems compliance with outage specifications is guaranteed for all bands. In fact, inspection of Fig. 2 shows that protection switching or mitigation may be necessary for all practical mean DGD and outage parameters as long as the hinge model applies. Handling the noncompliant bands also requires their identification while in service.

An alternative to Fig. 2 is shown in Fig. 3, where mean DGD and outage are used as axes and NCR values are shown as contours. This corresponds to the traditional way of depicting the relation between mean DGD and PMD outage [6]. The traditional curves for NRZ and RZ are shown dashed in Fig. 3, again indicating the values where there is an abrupt transition between NCR $= 0$ and NCR $= 1$. Note that the contours of constant NCR for the hinge model, shown for NRZ and RZ, are noticeably flatter in the outage range of interest $(10^{-4}$–$10^{-8})$ than the traditional outage curves, meaning that for a given NCR, small changes in mean DGD of the fiber link will lead to large changes in outage probability.

Fig. 4 shows a third way of depicting the three-way relationship, plotting NCR as a function of mean DGD with outage values shown as contours. The limit for zero outage shown dotted agrees well with our approximation for NCR_0. The close spacing of the curves re-emphasizes that only a small change in mean DGD is required to achieve large changes in outage probability. For example, for NRZ and for outages from 10^{-3} to zero, the transition of NCR from zero to one occurs over the range of mean DGD/T from 0.075 to 0.2.

In conclusion, for systems characterized by the hinge model, we have used outage maps to determine the relationship among mean fiber DGD, outage probability, and the fraction of the WDM fiber spectrum noncompliant with a specified outage. Whereas a finite number of hinges creates a fraction of "outage free" channels, a finite number of hinges does not allow a guarantee that all channels will have an outage probability below a certain specification.

ACKNOWLEDGMENT

The authors would like to acknowledge valuable discussions with P. Magill, N. Frigo, and A. Chraplyvy.

REFERENCES

[1] M. Karlsson, J. Brentel, and P. A. Andrekson, "Long-term measurement of PMD and polarization drift in installed fibers," *J. Lightw. Technol.*, vol. 18, no. 7, pp. 941–951, Jul. 2000.

[2] R. Caponi, B. Riposati, A. Rossaro, and M. Schiano, "WDM design issues with highly correlated PMD spectra of buried optical cables," in *Proc. Optical Fiber Communicaiton Conf. (OFC 2002)*, pp. 453–455.

[3] M. Brodsky, N. J. Frigo, and P. Magill, "Polarization-mode dispersion of installed recent vintage fiber as a parametric function of temperature," *IEEE Photon. Technol. Lett.*, vol. 16, no. 1, pp. 209–211, Jan. 2004.

[4] M. Brodsky, M. Boroditsky, P. Magill, N. J. Frigo, and M. Tur, "Channel-to-channel variation of non-Maxwellian statistics of DGD in a field installed system," in *Proc. Eur. Conf. Optical Communication (ECOC 2004)*, vol. 3, Paper WeI.4.1, pp. 306–309.

[5] M. Boroditsky, M. Brodsky, N. J. Frigo, P. Magill, C. Antonelli, and A. Mecozzi, "Outage probabilities for fiber routes with finite number of degrees of freedom," *IEEE Photon. Technol. Lett.*, vol. 17, no. 2, pp. 345–347, Feb. 2005.

[6] H. Kogelnik, L. E. Nelson, and R. M. Jopson, "Polarization mode dispersion," in *Optical Fiber Telecom. IVB*, I. P. Kaminow and T. Li, Eds. San Diego, CA: Academic, 2002, pp. 725–861.

[7] P. J. Winzer, H. Kogelnik, C. H. Kim, H. Kim, R. M. Jopson, L. E. Nelson, and K. Ramanan, "Receiver impact on first-order PMD outage," *IEEE Photon. Technol. Lett.*, vol. 15, no. 10, pp. 1482–1484, Oct. 2003.

[8] H. Bülow, "Operation of digital optical transmission system with minimal degradation due to polarization mode dispersion," *Electron. Lett.*, vol. 31, pp. 214–215, Feb. 1995.

[9] P. J. Winzer, H. Kogelnik, and K. Ramanan, "Precise outage specifications for 1st-order PMD," *IEEE Photon. Technol. Lett.*, vol. 16, no. 2, pp. 449–451, Feb. 2004.

[10] C. Antonelli and A. Mecozzi, "Statistics of the DGD in PMD emulators," *IEEE Photon. Technol. Lett.*, vol. 16, no. 8, pp. 1840–1842, Aug. 2004.

[11] H. Kogelnik, L. E. Nelson, and P. J. Winzer, "Second-order PMD outage of first-order compensated fiber systems," *IEEE Photon. Technol. Lett.*, vol. 16, no. 4, pp. 1053–1055, Apr. 2004.

[12] A. Mecozzi, C. Antonelli, M. Boroditsky, and M. Brodsky, "Characterization of the time dependence of polarization mode dispersion," *Opt. Lett.*, vol. 29, pp. 2599–2601, Nov. 2004.